

# A New Brain-Machine Interface Algorithm Based on Neural Firing: A Study Based on Modeling

Masoud Amiri <sup>1</sup>, Bahador Makkiabadi <sup>1</sup>, Amir Homayoun Jafari <sup>1</sup>, Soheila Nazari <sup>2\*</sup>

<sup>1</sup>Medical Physics & Biomedical Engineering Department, School of Medicine, Tehran University of Medical Sciences, Tehran, Iran.

<sup>2</sup>Faculty of Electrical Engineering, Shahid Beheshti University, Tehran, Iran.

## Abstract

In this paper, we develop a novel approach for bidirectional brain-machine interface (BMI). First, we propose a neural network model for sensory cortex ( $S_1$ ) connected to the neural network model of motor cortex ( $M_1$ ) considering the topographic mapping between  $S_1$  and  $M_1$ . We use 4-box model in  $S_1$  and 4-box in  $M_1$  so that each box contains 500 neurons. Individual boxes are composed of two neural populations: inhibitory interneurons and pyramidal neurons. Next, we develop a new BMI algorithm based on neural firing. The main concept of these BMI algorithm is to close the loop between two components: the sensory interface and the motor interface. The sensory interface encodes some of the state parameters of the external device into an electrical stimulus delivered to the  $S_1$  model. The motor interface takes neural recordings from the  $M_1$  model and decodes them into a force applied to the object. We present the simulation results for the on line BMI which means that there is a real time information exchange between the  $S_1$ - $M_1$  network model and the external device.

**Keywords:** Brain machine interface, neural firing, sensory and motor cortex.

\* Corresponding author

Email addresses: [so\\_nazari@sbu.ac.ir](mailto:so_nazari@sbu.ac.ir)

Received: April 2023

Revised: May 2023

## 1. Introduction

A long time has passed since the first demonstration of a robotic manipulator controlled by neuronal activity. The rising prospect of brain machine interfaces has since then seen a remarkable scientific revolution [Tiwari et al. 2020]. The idea of controlling robotic devices by brain activities has been driven by two different viewpoints. One is providing paralytic people with a “new channel to the world”. The other is to provide researchers in neuroscience with a new family of experimental tools to answer basic questions, such as how the known mechanism of neuroplasticity may provide the physiological foundation for learning and memory [Vato et la., 2014, Vato et la., 2012]. While in the last decade there have been significant advances on both perspectives, there are still practical and conceptual challenges which remain widely open.

The brain-machine interfaces (BMIs) are devices that decode neural activity, maintaining two main approaches: one is based on decoding as a proxy for the intended state of motion, or for muscle activations. The other view is based on decoding high-level motor goals from neural activity, and to communicate this goal to an artificial controller in charge of its execution. In both approaches, the focus is on decoding neural signals, and it has been only recently that attention has been devoted to the problem of electrical stimulation of the brain based on the machine movement position. Most BMI researchers typically consider controlling an external device based on decoding neural activity or play a computer game by the subjects. A motor BMI system consists of four basic elements: recording technology to extract brain activity, decoding algorithm to translate brain activity to the predicted movement of the external device, external device (prosthetic limb such as a robotic arm), and encoding interface to convert the motion of the external device to electrical stimulation of the brain. Therefore, in such controlling systems like BMI, feedback is an essential part of the system in developing the closed-loop brain-machine interface. Most current studies employ visual feedback to the subject for error correction and algorithm learning.

In Sensory BMIs, a direct connection pathway is considered from an external device, e.g. an artificial retina, to the nervous system; while in the bidirectional BMIs, a bi-directional direct communication is established between the nervous system and an external device. The former has been a subject of research for a longer time, and is primarily utilized to help a person communicate a message to his/her environment through an external device like a computer or prostheses, whereas the latter is more complicated, therefore also being a more recent subject. This kind of BMI might have the potential to restore motor function or impaired neural activity, by means of simply put helping to “retrain the brain” [Carmena, 2013]. The concept of bidirectional brain machine interfaces has been studied by Fetz [Moritz et al. 2008], Ivaldi [Ivaldi et al. 2010]. Ivaldi defines the bidirectional brain machine interface as “a fancy combination of neural decoding and simulation apparatus, connected via an artificial body” [Ivaldi et al. 2010]. Fetz proposed inducing plastic changes driven by sensorimotor interaction, however did not investigate the different techniques to accomplish his proposition [Jackson and Fetz, 2011]. Figure 1 shows the bidirectional BMI. In this setup, the sensory information about the current state of the external system was conveyed to the neural preparation by means of electrical pulse trains of variable frequencies,

delivered by electrode to  $S_1$ . Population spike trains extracted in real time from extracellular multiunit recording from  $M_1$  were transformed into a control signal used to drive the external system. Indeed, the main idea of the bidirectional BMI algorithm is the transformation of information about the state of the device into brain activity using electrical stimulation and then decoding of motor cortical activity into a set of forces needed to accomplish the task such as reaching a target.

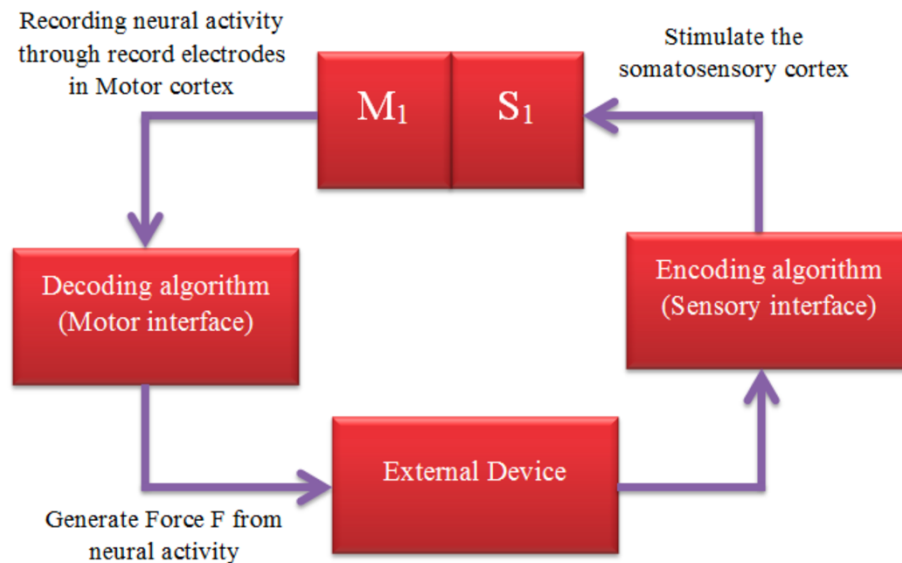


Figure 1. The bidirectional BMI. The recording and stimulating arrays are placed on the motor ( $M_1$ ) and sensory areas ( $S_1$ ) of the cortex, respectively.

In this research, we address the bidirectional BMI from a modeling point of view. We begin by simulating the primary somatosensory cortex ( $S_1$ ) and vibrissal motor cortex ( $M_1$ ) with a sparsely connected network of excitatory and inhibitory neurons modeling a local cortical population. The model used for both  $S_1$ - $M_1$  is a 4- box model with a distant dependent connectivity among boxes. Individual box is composed of 400 pyramidal neurons and 100 interneurons. Then, by considering the topographic mapping, the  $S_1$ - $M_1$  network model is developed. In this way, it is supposed that one micro wire array delivers the micro stimulation to the  $S_1$  model and the second micro wire array records the neural signals from  $M_1$  model. Next, a novel BMI algorithm is introduced to control the motion state of a simulated point mass in a viscous medium toward a target region.

This algorithm uses the total number of firings to determine the position of our medium. The main idea of this algorithm is to close the loop between two components: the sensory interface and the motor interface. The sensory interface encodes the position of the point mass into an electrical stimulus delivered to the  $S_1$  model. The motor interface takes neural recordings from the  $M_1$  model and decodes them into a force applied to the device, which leads to evolve to the next position. The brain is informed about the new position by the sensory interface and generates a new motor cortical response.

The rest of the paper is organized as follows: Section 2 introduces the  $S_1$ ,  $M_1$  models to create a  $S_1$ - $M_1$  network. The BMI algorithm is explained in Section 3. The simulation results are discussed in Section 4 and Finally Section 5 concludes the paper.

## 2. Neural Network Model

To understand the rules of translation between the sensory stimuli and the fluctuations of cortical responses, a connected network of excitatory and inhibitory neurons are simulated. In this Section, we first explain the network model that is used for Sensory cortex ( $S_1$ ), next the neural model of Motor cortex ( $M_1$ ) and then its connection to the  $S_1$  model are described.

### 2.1. The $S_1$ network model

The  $S_1$  network model is composed of leaky integrate-and-fire neurons and is based on the model developed by [Mazzoni et al.,2008]. Figure 2 shows the main components of the network.

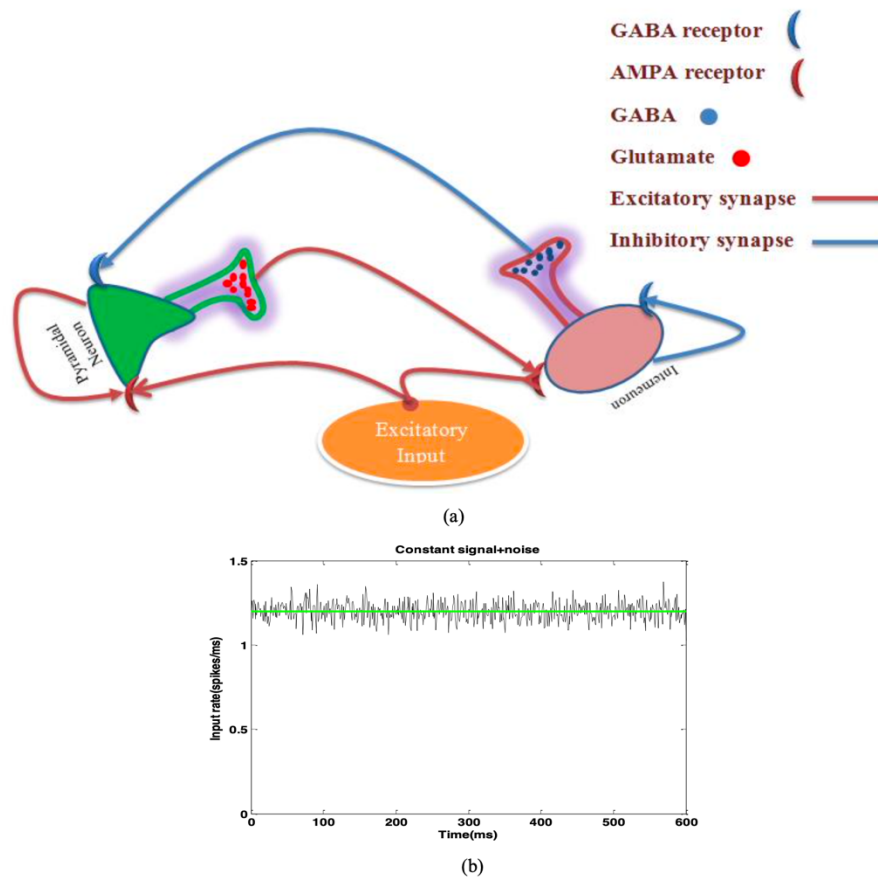


Figure 2. (a) The main components of the network which are interneurons, pyramidal neurons and excitatory and inhibitory synapses. (b) A time-varying rate of Poissonian spike trains as an input to network which average value is 1.2 spikes/ms.

The model network represents in a very simplified way a local circuit in S<sub>1</sub> cortex, and are composed of two neuronal populations: inhibitory interneurons and pyramidal neurons. The network connectivity was random and sparse with a 0.1 probability of directed connection between any pair of neurons. Synaptic activities are composed of AMPA currents (excitatory synaptic activities) and GABA currents (inhibitory synaptic activities). In order to simulate the activity from afferents, excitatory and inhibitory neural populations are excited using noisy external input.

We partition the S<sub>1</sub> model into four boxes (2 by 2). Inside each box, there are 100 interneurons and 400 pyramidal neurons. So, the total number of neurons for 4-box model are 2000 neurons. The membrane potential of neuron  $k$  is formulated as follows:

$$\tau_m \frac{dv_k}{dt} = -v_k + I_{AK} - I_{GK}, \quad (1)$$

where membrane time constant, excitatory (AMPA type) synaptic currents, and inhibitory (GABA-type) currents received by neuron  $k$  are denoted by  $\tau_m$  (20 ms for excitatory neurons, 10 ms for inhibitory neurons),  $I_{AK}$ ,  $I_{GK}$ , respectively. In Eq. 1 the resting potential and threshold are considered zero and 18 mV, respectively. Synaptic currents are the linear sum of contributions induced by single pre-synaptic spikes, which are described by a difference of exponentials. They can be obtained using auxiliary variables  $x_{AK}$ ,  $x_{GK}$ . AMPA and GABA-type currents of neuron  $k$  as follows:

$$\tau_{dA} \frac{dI_{Ak}}{dt} = -I_{Ak} + x_{AK}, \quad (2)$$

$$\tau_{rA} \frac{dx_{Ak}}{dt} = -x_{AK} + \tau_m \left( J_{k-pyr} \sum_{pyr} \delta(t - t_{k-pyr} - \tau_L) + J_{k-ext} \sum_{ext} \delta(t - t_{k-ext} - \tau_L) \right), \quad (3)$$

$$\tau_{dG} \frac{dI_{Gk}}{dt} = -I_{Gk} + x_{GK}, \quad (4)$$

$$\tau_{rG} \frac{dx_{AG}}{dt} = -x_{AG} + \tau_m \left( J_{k-int} \sum_{int} \delta(t - t_{k-int} - \tau_L) \right). \quad (5)$$

The values of parameters are taken from [Mazzoni et al.,2008]. The external excitatory input by random Poisson spike trains (in the form of time varying rate) identically is fed to each excitatory and inhibitory neuron by the following equation:

$$v_{ext}(t) = [v_{signal}(t) + n(t)]_+, \quad (6)$$

where  $v_{signal}(t)$  represents the signal, and  $n(t)$  is the noise. [...] is a threshold-linear function,  $[x]_+ = x$  if  $x > 0$ ,  $[x]_+ = 0$  otherwise. A stochastic variable,  $n(t)$  based on Ornstein-Uhlenbeck process is defined as follows:

$$\tau_n \frac{dn(t)}{dt} = -n(t) + \sigma_n \left( \sqrt{\frac{2}{\tau_n}} \right) \eta(t), \quad (7)$$

where  $\sigma_n$  is the standard deviation of the noise, and  $\eta(t)$  is a Gaussian white noise.

Individual boxes are connected with a function of the form  $K \exp\left(\frac{-R^2}{3.5}\right)$ , where  $K$  is a scaling factor and  $R$  is the distance between different boxes. The connectivity pattern of the 2000 neurons (4-box model) is shown in Figure 3.

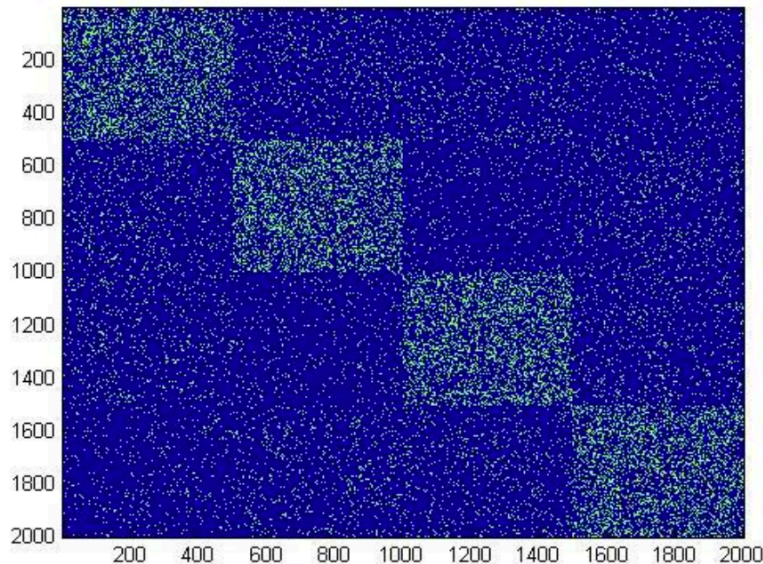


Figure 3. 100 interneurons and 400 pyramid neurons create each box of neural network as  $S_1$  model. The connection between any pair of neurons in each box is random with probability 0.1.

We quantified the neural activity by monitoring the spike activity of the individual neuron which is called 'firing rate' (this measurement is obtained by counting the number of spikes fired by neurons in a 1 ms bin), and the average synaptic currents [Logothetis 2003, Kamondi et al.,1998].

Figure 4 demonstrates the spiking behavior of the system with different rates of the input signal (1.2 and 2 spikes/ms). Raster plots in Figure 4 (a),(b) show that the neuronal firing was sparse in all conditions. Though spiking activity of single cells was seemingly random, inspection of the total firing rate from the pyramidal and the interneuronal population Figure 4(a),(b) showed that increasing the input signal rate causes an increasing average firing rate in the neural activities and consequently appearing synchronous spiking patterns in network activity.

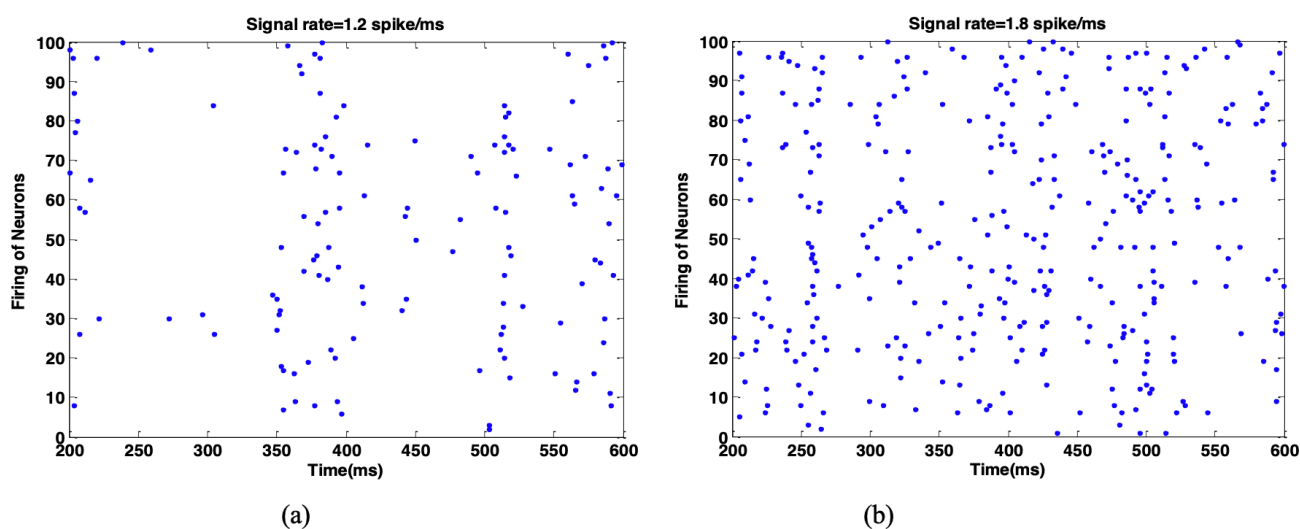


Figure 4. Dynamics of the network receiving a signal, box #3 of the 4-box  $S_1$  model, with two different rates (left column: 1.2 and right column: 2 spikes/ms), superimposed to noise. In each column, all panels show the same 400 ms interval (extracted from a 1 seconds simulation). (a), (b) Raster plot of the activity of 100 randomly selected pyramidal neurons.

## 2.2. The $M_1$ network model

The  $M_1$  network model is similar to the  $S_1$  model and it is also composed of a population of interneurons and pyramidal neurons except that we slightly changed the parameters values to have two different models. For the 4-box  $S_1$  model, we developed the 4-box  $M_1$  model. Fig.5 shows the dynamics of the same box of Fig.4 for the  $M_1$  network model.

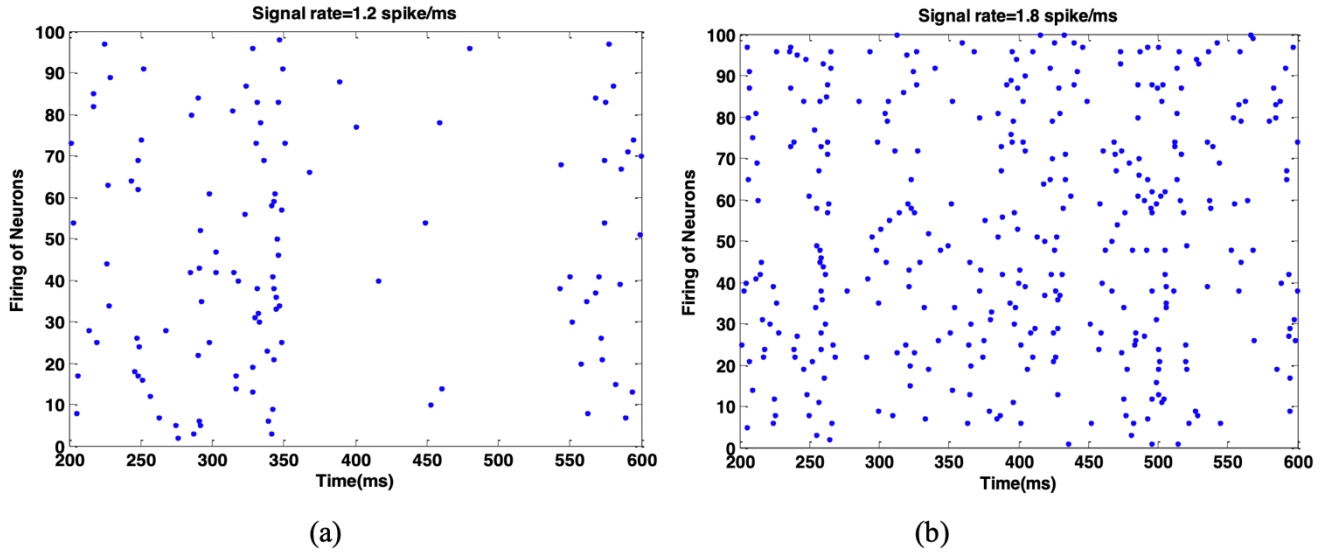


Figure 5. Dynamics of the neuronal network, box #2 of the 4-box M1 model, receiving a signal with two different rates (left column: 1.2 and right column: 2 spikes/ms), superimposed to noise. In each column, all panels show the same 400 ms interval (extracted from a 1 seconds simulation). (a) , (b) Raster plot of the activity of 100 randomly selected pyramidal neurons.

### 2.3. The S<sub>1</sub>-M<sub>1</sub> network model

Some experimental observation proved that a focal activation of S<sub>1</sub> causes a relatively localized activation of M<sub>1</sub> [Fries et al.,2001; Geisler et al.,2005; Gil and Amitai ,1996, Li et al. 2019]. In order to simulate the similar situation, each box of the S<sub>1</sub> is connected to the corresponding box of M<sub>1</sub>. This means that  $i^{\text{th}}$ -box of S<sub>1</sub> is connected to  $i^{\text{th}}$ -box of M<sub>1</sub>. A connecting coefficient based on mean firing rate of pyramidal neurons of each box of S<sub>1</sub> ( $K * \langle FR \rangle_{PY}$ ) is added to the corresponding box of M<sub>1</sub> as excitatory input. Therefore, Eq. (6) for  $i^{\text{th}}$ -box of M<sub>1</sub> is enhanced as follows:

$$v_{ext-ith-box-M_1}(t) = [v_{signal}(t) + n(t)]_+ + K * \langle FR \rangle_{PY,ith-box-S_1}. \quad (8)$$

In the model, we assume that the excitation and recording electrodes have the same number and shape in the corresponding regions of S<sub>1</sub> and M<sub>1</sub>. So that when a stimulus occurs in an area of S<sub>1</sub>, this stimulus is sensed at the corresponding recording electrode of M<sub>1</sub>, and this interaction is also observed in real data [Geisler et al.,2005].

In the simulation process, by moving the stimulus electrodes, we create the excitation in different areas of  $S_1$ . Considering Figure 6 one can notice that the total firing rate increases for that box of  $M_1$  corresponding to the stimulated box of  $S_1$  and there is a gradient in the recorded activities of  $M_1$  network. This helps to consider a total firing rate as a feature for bidirectional brain-machine interface. This issue will be explained in detail the subsequent sections.

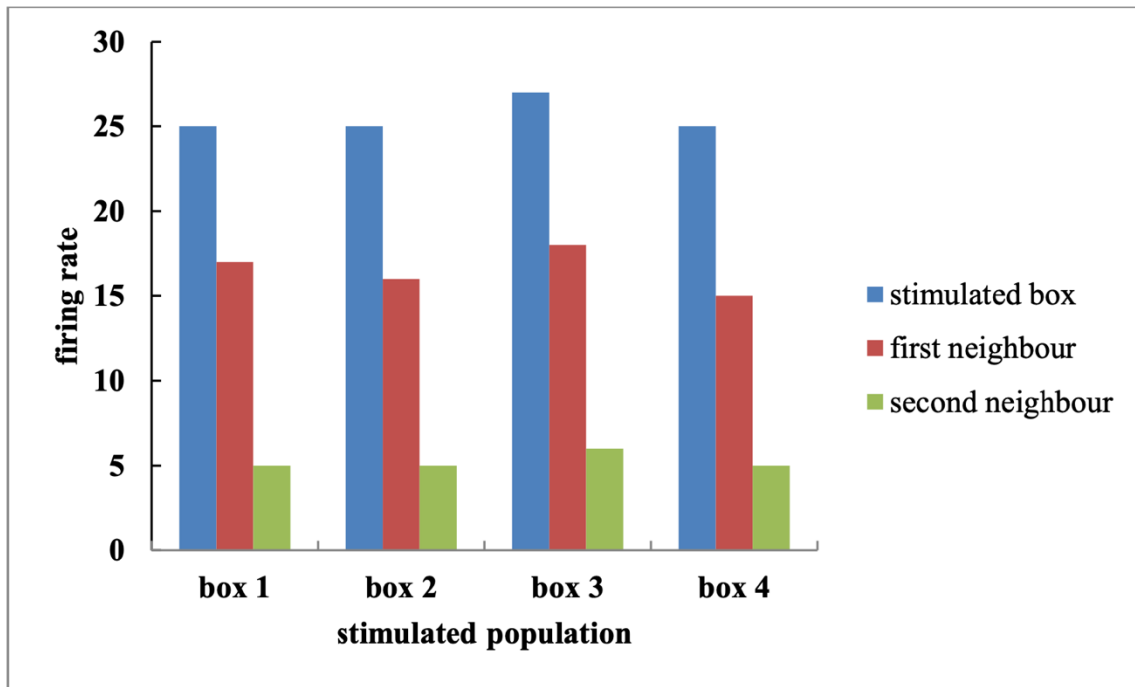


Figure 6. Firing rate of randomly selected 5 neurons from each box of  $M_1$  per sensory stimulation. In this simulation, we used a 4-box model for  $S_1$  and  $M_1$ . It is assumed that both stimulating and recording electrodes are arranged in a  $2 \times 2$  grid. Due to a distant dependent connectivity among neurons in  $S_1$  and  $M_1$ , stimulating 4 different electrodes (boxes) of  $S_1$ , one by one, yields a gradient in the evoked spikes in  $M_1$ .

### 3. BMI algorithm

In the BMI by closing the loop between sensory cortex and motor cortex, the artificial hand (external device) will be able to control. The sensory interface maps some of the state parameters of the external device such as position of the end point into one of a set of electrical stimulation delivered to a cortical sensory area. The result of this operation is that the activity evoked in this sensory area encodes the state parameters of the device. The role of the motor interface is to record neural activity from a motor-cortex region and translate it into a force for moving the external device. Hence, the device evolves to the next state. The new position is received by the sensory area and converted into a stimulus and subsequent

motor response, which again leads to the production of new force and movement of the artificial limb, and this loop is repeated until the external device reaches the target location.

A set of sensory stimuli and spike responses received from the motor cortex are used as calibration data to determine the sensor parameters and zoning of the artificial limb movement space. Then the ability of the closed loop BMI algorithm in the interaction of sensory and motor for controlling the movement of robotic arm is evaluated.

In fact, the BMI algorithm based on the maximum Firing rate as decoding algorithm, calibrate sensory interface in movement of external device according to the desired force field of Figure 7. The force field  $\phi(x)$  is a force which is applied to the external device in the coordinates of  $x$  as follows:

$$\phi(x) = K(x)(x - 60)(x + 60). \quad (9)$$

Figure 7 indicates the desired force field which can control device movement toward an equilibrium state in the origin.

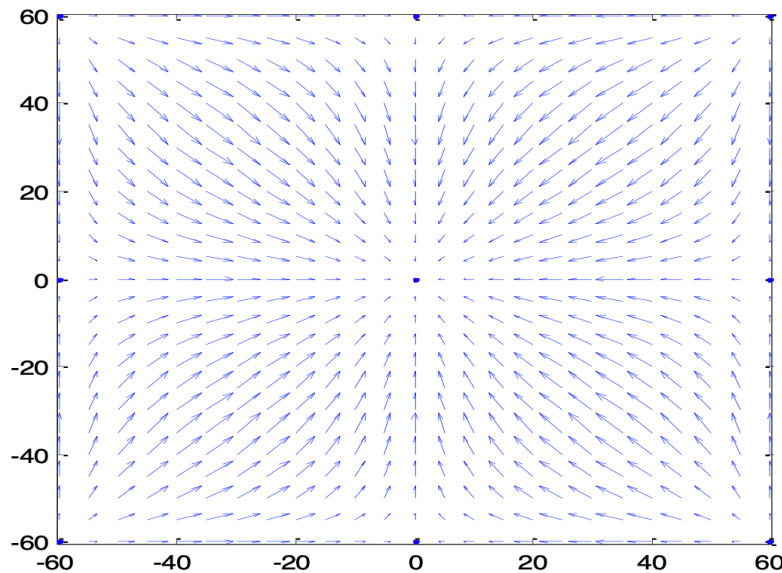


Figure 7. The desired force field in sensory interface.

In fact, the trajectories in Figure 7 show the mechanical arm that is supposed to move toward the center on the plane (sensory interface).

In the simulation steps of the BMI algorithm test, the mechanical arm starts moving from the initial position  $x_0$  at zero velocity on the sensory interface plane. The initial position  $x_0$  through Eq.10 (the

encoding algorithm) and corresponding to the area of the external device in sensory interface is converted to electrical stimulus  $\tilde{s}$ :

$$\tilde{s} = \operatorname{argmin}(\|x_0 - \xi_i\|), \quad i = 1, \dots, M \quad (10)$$

where, the center of each region in sensory interface and number of simulation patterns are denoted by  $\xi_i$  and  $M$ , respectively. The encoding algorithm provide stimulus  $\tilde{s}$  to excite  $S_1$  model and consequently, spiking response  $\tilde{r}$  from the  $M_1$  can be recorded. In the next step, the motor interface or the decoding algorithm converts the recorded spike  $\tilde{r}$  into force. Then the calculated force is applied to the mechanical arm and we allow the arm to move at a fixed time interval and reach position  $x_1$ , and finally this loop will continue. When external device reaches the target region, the algorithm converges, and when the number of iterations of the algorithm exceeds the maximum iterations (40), the algorithm diverges. Operating the simulation steps of the algorithm test requires calibration of the sensory interface, which is described in the next section.

### 3.1 Calibration of the sensory interface

In proportion to the electrical stimulation, a map is created from the position of the mechanical system so that the sensory interface can be calibrated. The final product is to partition of the position space of the external device into a set of *sensory regions*, such that each being associated to a particular electrical stimulus. The following is a detailed description of the sensory interface calibration.

Assume that a set of electrical stimuli  $s = \{s_1, s_2, \dots, s_M\}$  should be applied. Consequently, a set of recording spike from motor cortex in response to each electrical stimulus obtain which called “*calibration responses R*”:

$$R = [r_{i,j}], \quad i = 1, \dots, M; \quad j = 1, \dots, N \quad (11)$$

Each response,  $r_{i,j}$  consists of a sequence of spike times for each of the recorded neurons in a simulated 0-600 ms post-stimulation window. We implemented algorithm that translate the current response  $r$  into a point in the position space of the mechanical system.

As is evident from Figure 6, among firing rate of the recorded spikes from each box of  $M_1$  model, there is a gradient. So in the decoding algorithm, we simply sum the number of spikes recorded from 5 selected neurons in each  $M_1$ -boxes for individual trials. In this way, we create an  $A$  matrix whose its elements are the total number of firings of individual box:

$$A = [a_{p,q}], \quad p = 1, \dots, M \times N; \quad q = 1, \dots, M \quad (12)$$

Then the symmetric distance matrix  $D = [d_{k,l}]$  obtained by calculating the Euclidean distance between the data of matrix  $A$  is calculated. Therefore, distance matrix  $D$  is formed based on total firing. Using multi-dimensional scaling function in MATLAB, matrix  $D$  which is based on distance of total firing is clustered:

$$x = [x_{i,j}], \quad [x_{i,j}] = [x_{1,i,j}, x_{2,i,j}]^T, \quad (13)$$

where  $i, j$  are proportional to the dimensions of  $M$  and  $N$ , respectively. The obtained locations are multiplied by a fixed factor  $f$  in order to fit the movement space with dimensions of  $100 \times 100$  (the position space is shown in Figure 8):

$$\tilde{x} = [\tilde{x}_{i,j}] = f \cdot x \quad (14)$$

Finally, by averaging the points of each cluster, the centers of the clusters are calculated:

$$\xi_i = \frac{1}{N} \sum_{j=1}^N \tilde{x}_{i,j}, \quad i = 1, \dots, M \quad (15)$$

Using the obtained  $M$  cluster centers and the nearest neighbor algorithm, the movement space is divided into  $M$  regions as shown in Figure 8(b). Figure 8 shows the sensory regions for the 4-box model of  $S_1$ - $M_1$  network, which is the calibration of the sensory interface using the total firing rate. For these simulations, we stimulate each box 20 trails with different noise realization and then record 5 randomly selected neurons from individual boxes. In this configuration, each stimulation pattern was constituted by the activation of only one of the stimulating electrodes (box). This figure is in line with Figure 6, which previously showed the topographic mapping for the 4-box  $S_1$ - $M_1$  network model. Since we have 4 stimuli and 20 trials, we will have 4 sets (cluster of points) which contains 20 points, which obtained by projecting the distance matrix,  $D$ , into in 2-dimensional space using MDS. Then, applying nearest neighbor algorithm, the sensory map is created. The calibration centers were showed as a square in data points and colored regions. As this figure illustrates, the BMI algorithms create 4 distinct regions and it has a good performance.

The within-class scatter matrix ( $S_W$ ) and between class scatter matrix ( $S_B$ ) which define Class Scatter Measure (CSM (J)) was used to qualify the performance of the proposed algorithm to classify the data into four classes:

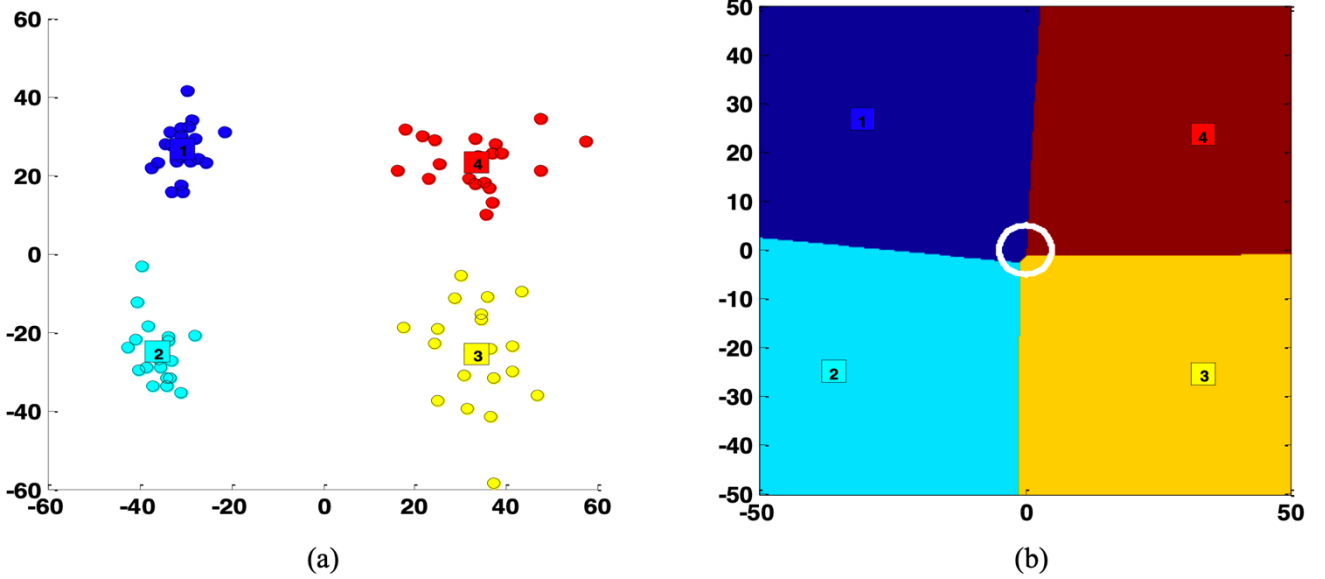


Figure 8. Results of the calibration of sensory interface using the total firing algorithms. The goal of the calibration procedure is to define the sensory regions by partitioning the position space of the controlled device. Here, we used a 4- box  $S_1$ - $M_1$  network model and each time we stimulated one box, 20 times with different noise realization and hence we have 4 sets (cluster of points) which contains 20 points. (a): projecting the distance matrix,  $D$ , into in 2-dimensional space using MDS and (b) show the sensory regions obtained using a nearest neighbor algorithm. The squares show the centers of clusters.

$$S_W = \sum_{i=1}^c \left[ \sum_{j=1}^{n_i} (x_{i,j} - m_i)(x_{i,j} - m_i)^T \right], \quad (16)$$

$$S_B = \sum_{i=1}^c n_i (m_i - m)(m_i - m)^T, \quad (17)$$

$$J = \frac{S_B}{S_W}. \quad (18)$$

The number of classes, number of samples in  $i$ -th class, the  $j$ -th sample in the  $i$ -th class, mean of samples in the  $i$ -th class and mean of all samples are denoted by  $c, n_i, x_{i,j}, m_i, m$ , respectively. In Table 1 we show CSM for simulation data. Large values of  $J$  are desirable because distance between-class is large and within-class is low.

Table 1: CSM for simulation data

DATA	CSM (J)
Simulation data	1.104

### 3.2 The motor interface

The motor interface as decoding algorithm converts the recorded spike response  $\tilde{r}$  from  $M_1$  into a force, which can drive the external device along the target region with the following dynamical equation:

$$M \cdot \ddot{x} + B \cdot \dot{x} = F, \quad (19)$$

where  $F$  is the force obtained from the neural response using motor interface,  $B = 13 \text{ N} \cdot \text{s}/\text{m}$  is a force due to the viscosity  $x = [x_1, x_2]^T$ , is the position of the trajectories as external device on a plane and  $M = 10 \text{ Kg}$  is the device weight. Eq. 19 was solved based on Runge-Kutta algorithm to calculate the new position  $x$  of external device after applying the force  $F$ .

To map current response  $\tilde{r}$  into a force, we calculate the distances between the currently recorded  $\tilde{r}$  and all the responses in the calibration trials. These distances are stored in a matrix  $\tilde{D}$ :

$$\tilde{D} = [\tilde{d}_{i,j}], \quad i = 1, \dots, M, \quad j = 1, \dots, N \quad (20)$$

Following [Vato et al., 2014, Vato et al., 2012], we compute the average of the distances  $\tilde{d}_{avg}^i$ , and then decode the stimulus  $\tilde{s}_{dec}$  whose calibration responses gave the smallest average distance

$$\tilde{s}_{dec} = \operatorname{argmin}_i(\tilde{d}_{avg}^i), \quad i = 1, \dots, M \quad (21)$$

The force vector applied to the external device is the same as the force value given by the force field at the position of the calibration center corresponding to the decoded stimulus:

$$F = \phi(x_v), \quad \text{with } x_v = \xi_{\tilde{s}_{dec}}. \quad (22)$$

## 4. Results

As explained in the previous sections, we proposed 4-box models for the  $S_1$ - $M_1$  network. Next, we explained the neural firing BMI algorithm and also the sensory/ motor interfaces (encoding/decoding

parts) were described. Now, in this section, we want to use the BMI algorithm based on total firing to create the closed loop interaction between the external device (reaching the target region) and the  $S_1$ - $M_1$  network model.

As described, the motor interface decodes the recovered responses from the  $M_1$  model to the propulsive force of the external device, and the sensory interface encodes the new position of the external device to the stimulus applied to the  $S_1$  model. In this section, the online information exchange between  $S_1$ - $M_1$  network model and external device through the BMI algorithm is reported.

We test the BMI algorithm 16 times with 16 different starting points on the sensory plane. The external device is guided from the initial point  $x_0$  to the target area (white circle in Figure 9) using the proposed BMI algorithm with the calibrated sensory interface of Figure 8.

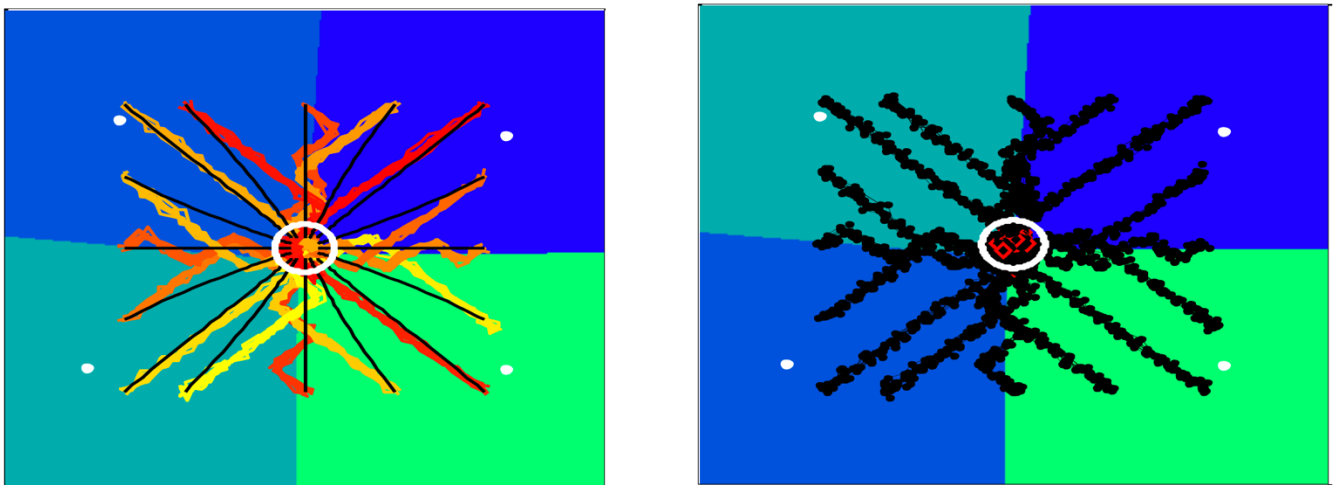


Figure 9. Performance of the on line BMI algorithms by using the total firing rate algorithm for 4-box model of  $S_1$ - $M_1$  network.

The left panel of Figure 9 shows the trajectories (denoted external device) of the system for the 4-box  $S_1$ - $M_1$  network model, starting from 16 different initial positions. The colored lines and black lines denoted trajectories generated by closed loop BMI algorithm and ideal trajectories, respectively. Also, the right panel of Fig.9 indicates the step by step trajectories movement in the closed loop interaction between external device and  $S_1$ - $M_1$  network model. As it is evident, the BMI algorithm has succeeded in controlling the movement of the mechanical arm towards the target area. The simulation results presented in Figure 9 have been repeated 10 times to show the robustness of the algorithm, and the results confirm the robustness of the closed loop BMI protocol. In order to quantify the performance accuracy of the algorithm in guiding the mechanical arm towards the target area, we introduced a

criterion called Within-trajectory position error (WTPE) which calculates the distance between ideal and actual trajectories in the left panel of Figure 9. The WTPE parameter is obtained 4.2958 for 10 repetitions of BMI algorithm. Also, the average number of steps in reaching trajectories to the target region in 10 iterations of the algorithm is 26, which indicates the good performance of the closed loop BMI algorithm.

## 5. Conclusion

In recent years, the development of BMI algorithms to help people with neurological deficits has been highly considered. In the closed-loop BMI system (bidirectional BMI), control a mechanical device and constructing artificial sensory information about the position of an external device are based on the recording neural signal from the motor areas and electrical stimulation of sensory areas, respectively. In general, to implement a closed-loop BMI system in a portion of the nervous system, an encoding, and decoding algorithm can be implemented by micro-stimulation techniques and neural activity recording, respectively. In this regard, we designed a bidirectional BMI by simultaneously controlling encoding and decoding interfaces. We modeled the primary somatosensory cortex ( $S_1$ ) and vibrissal motor cortex ( $M_1$ ) as a population of inhibitory interneurons and excitatory pyramidal neurons with AMPA and GABA synapses. Next, these two networks were connected to create the  $S_1$ - $M_1$  network model. Then, the BMI algorithm based on neural firing was proposed. Indeed, the motor interface part of these algorithms decoded the evoked activity of the recorded motor cortical neurons ( $M_1$  model) into a force vector applied to the point mass in a viscous medium. The sensory interface part encoded the position of the point mass into a stimulus delivered to the somatosensory cortex ( $S_1$  model). Finally, we presented the results of applying the total firing rate algorithm, from the computational point of view, on the simulation data recorded from  $M_1$  in response to electrical stimulation of  $S_1$ . The simulation results illustrate the effectiveness of the proposed BMI algorithm.

## Reference:

Carmena, J. M. (2013). Advances in neuroprosthetic learning and control. *PLoS biology*, 11(5), e1001561.  
Fries P, Reynolds JH, Rorie AE, deSimone R (2001) Modulation of oscillatory neuronal synchronization by selective visual attention. *Science* 291: 1560–1563.

Geisler C, Brunel N, Wang XJ (2005) Contributions of intrinsic membrane dynamics to fast network oscillations with irregular neuronal discharges. *J Neurophysiol* 94: 4344–4361.

Gil Z, Amitai Y (1996) Properties of convergent thalamocortical and intracortical synaptic potentials in single neurons of neocortex. *J Neurosci* 16: 6567–6578.

Kamondi A, Acsadi L, Wang XJ, Buzsaki G (1998) Theta oscillations in somata and dendrites of hippocampal pyramidal cells in vivo: activity-dependent phaseprecession of action potentials. *Hippocampus* 8: 244–261.

- Li, W., Li, C., Xiang, Y., Ji, L., Hu, H., & Liu, Y. (2019). Study of the activation in sensorimotor cortex and topological properties of functional brain network following focal vibration on healthy subjects and subacute stroke patients: An EEG study. *Brain research*, 1722, 146338.
- Logothetis NK (2003) The underpinnings of the bold functional magnetic resonance imaging signal. *J Neurosci* 23: 3963–3971.
- Mazzoni, A., Panzeri, S., Logothetis, N. K., & Brunel, N. (2008). Encoding of naturalistic stimuli by local field potential spectra in networks of excitatory and inhibitory neurons. *PLoS Comput Biol*, 4(12), e1000239.
- Vato A, Semprini M, Maggiolini E, Szymanski FD, Fadiga L, et al. (2012) Shaping the dynamics of a bidirectional neural interface. *PLoS Comput Biol* 8: e1002578
- Jackson, A., & Fetz, E. E. (2011). Interfacing with the computational brain. *Neural Systems and Rehabilitation Engineering, IEEE Transactions on*, 19(5), 534-541.
- Moritz, C. T., Perlmutter, S. I., & Fetz, E. E. (2008). Direct control of paralysed muscles by cortical neurons. *Nature*, 456(7222), 639-642.
- Mussa-Ivaldi, F. A., Alford, S. T., Chiappalone, M., Fadiga, L., Karniel, A., Kositsky, M., ... & Vato, A. (2010). New perspectives on the dialogue between brains and machines. *Frontiers in neuroscience*, 4.
- Vato, A., Szymanski, F. D., Semprini, M., Mussa-Ivaldi, F. A., & Panzeri, S. (2014). A bidirectional brain-machine interface algorithm that approximates arbitrary force-fields. *PloS one*, 9(3), e91677.
- Tiwari, N., Edla, D. R., Dodia, S., & Bablani, A. (2018). Brain computer interface: A comprehensive survey. *Biologically inspired cognitive architectures*, 26, 118-129.